Journal of Sound and Vibration (2000) **238**(1), 1–18
doi:10.1006/jsvi.2000.3099, available online at http://www.idealibrary.com on IDEAL®

THE EFFECTS OF CLOSURE OF CRACKS ON THE DYNAMICS OF A CRACKED CANTILEVER BEAM

M. KISA AND J. BRANDON

Division of Mechanical Engineering and Energy Studies, Cardiff School of Engineering, University of Wales, Cardiff, P.O. Box 685, *Cardiff CF*2 3*TA, England. E-mail: brandon@ef.ac.uk*

(*Received* 3 *February* 1998, *and in final form* 28 *March* 2000)

The paper develops a finite element scheme for computing the eigensystem for a cracked beam for different degrees of closure. Previous work in the authors' laboratories has indicated that the ability to extend the use of mode superposition to model breathing conditions in the crack zone would overcome the need to switch from a frequency-domain-based model to a time-stepping scheme which had caused both implementational and theoretical problems. In this study, the finite element method, the component mode synthesis method and the linear elastic fracture mechanics theory are integrated for modelling of the cracked structures. It is believed that this is a novel synthesis of methods. The method used by the authors is benchmarked against earlier results in the literature.

1. INTRODUCTION

In recent years, vibration-based inspection has become an effective and fast method for detecting structural defects, such as cracks [1, 2]. In principle, the position and scale of the defect can be determined from changes in natural frequencies [3], mode shapes of vibrations [4] and also amplitudes of forced response [5]. It has been shown that a crack in a structure such as a beam may cause the structure to exhibit non-linear behaviour if the crack opens and closes ("breathes") during the vibration. However, in the most commonly used model it is assumed that the crack is fully open during vibration. When a crack opens and closes during vibration, contact phenomena must be taken into account.

Closing or breathing cracks have been investigated by Carlson [6] and Gudmunston [7], who studied the effects of closing cracks on the dynamical characteristics of an edge-cracked cantilever beam. Gudmunston found that the relative increase in natural frequencies caused by a closing crack is much smaller than the decrease due to an open crack when compared to the equivalent intact beam. Later, this experimental work was confirmed, using a numerical integration method, by Ibrahim *et al.* [8] who, in their study, modelled a crack as a bilinear spring.

Chen and Chen [9], Actis and Dimarogonas [10], and Collins *et al.* [11] studied the longitudinal free and forced vibrations of a prismatic bar by using direct numerical integration through the Galerkin method. Friswell and Penny [12] used a simplistic model of the non-linear behaviour of a beam with a closing crack.

Gash *et al.* [13] and Papadopoulos and Dimarogonas [14] studied the instability of rotors due to closing cracks. They used a local flexibility to model the changes of the

cracked rotor. Zastrau [15], using the finite element method, investigated the steady state responses of a simply supported beam with multiple closing cracks. Qian [16] observed that the differences between amplitudes of forced vibrations of cracked beams are reduced when the closing crack model is considered. Ostachowitz and Krawczuk [17], by using special local finite elements in the contact area, studied the influence of a closing crack. In a recent paper, these authors presented an analysis of the forced vibrations of a cantilever beam with a closing crack, in which the equations of motion were solved using the harmonic balance method [18].

It is important to realize that many of the finite element methods used to model damaged structures are either section reduction or material property degradation methods and are not non-linear crack section methods. It should be noted that a number of authors make no distinction between an intact beam and the limiting stiffness as a crack depth tends to zero. In the dynamic problem this distinction is important. (See, for example, the commentary in the paper by Abraham and Brandon [19]).

Abraham and Brandon applied a piece-wise linear approach to analyze vibrations of a cantilever beam with a "breathing crack". Their formulation was a hybrid frequency-domain/time-domain method. For the majority of the vibration, the crack section is unambiguously either open or closed. During this time a mode superposition is used to develop the response of the system. Once an imminent transition is predicted it is necessary to transform to the time domain to model the contact conditions. This switching procedure (described in the appendix to the paper by Brandon and Abraham [20]) was difficult to implement and used excessive computer time. It was recognized, although not implemented, that it was theoretically possible to model the breathing conditions using a succession of low-rank transformations between modal models, thereby enabling the synthesis of simulations wholly within the frequency domain. The current paper provides the methods and illustrative results to provide the basis for the assembly of a fully non-linear model using successive modal transformations.

2. MATHEMATICAL MODEL

In Figure 1, a cantilever beam, of uniform cross-section A, having a transverse edge crack of depth a at a variable position ξ, is shown.

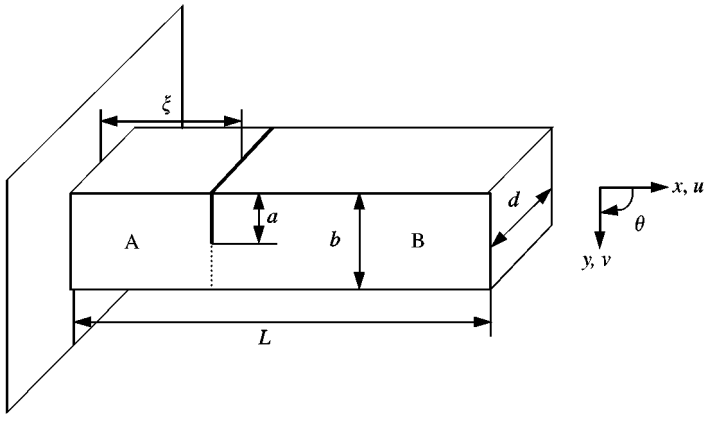

Figure 1. Geometry of the cracked cantilever beam.

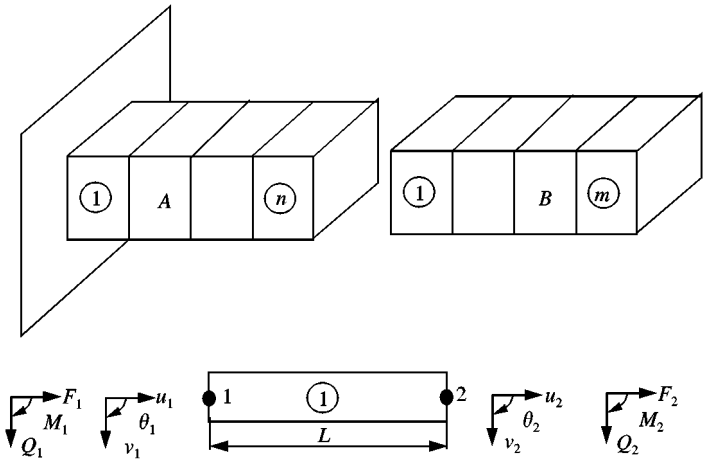

Figure 2. Components of the whole structure and the division into finite elements.

The cantilever is partitioned into two components (A and B) at the crack section enabling a substructure approach. By separating the whole beam into two parts, the global non-linear system can be separated into two linear subsystems joined by a local stiffness discontinuity. In the current study, each component is also divided into finite elements with two nodes and three degrees of freedom (d.o.f.s) at each node as shown in Figure 2.

2.1. STIFFNESS AND MASS MATRICES FOR CANTILEVER BEAM ELEMENT

The stiffness and mass matrices are developed from the procedure given by Petyt [21] adapted to 3 d.o.f.s for each node, $\delta = \{u, v, \theta\}$. As can be seen in Figure 2, representing a general finite element, the applied system forces $F = \{F_1, Q_1, M_1, F_2, Q_2, M_2\}$ and the corresponding displacements are shown $\delta = \{u_1, v_1, \theta_1, u_2, v_2, \theta_2\}$. The stiffness and mass matrices for a two-noded cantilever beam having two nodes with 2 d.o.f.s $\{v, \theta\}$at the each node, for bending in the xy plane, are given by Petyt as

$$[K_1] = \frac{EI_z}{2k^3(1+3\beta)} \begin{bmatrix} 3 & 3k & -3 & 3k \\ 3k & (4+3\beta)k^2 & -3k & (2-3\beta)k^2 \\ -3 & -3k & 3 & -3k \\ 3k & (2-3\beta)k^2 & -3k & (4+3\beta)k^2 \end{bmatrix} \tag{1}$$

and

$$[M_1] = \frac{\rho Ak}{210(1+3\beta)^2} \begin{bmatrix} m_1 & m_2 & m_3 & m_4 \\ m_2 & m_5 & -m_4 & m_6 \\ m_3 & -m_4 & m_1 & -m_2 \\ m_4 & m_6 & -m_2 & m_5 \end{bmatrix}$$

$$+\frac{\rho I_z}{30k(1+3\beta)^2}\begin{bmatrix} m_7 & m_8 & -m_7 & m_8 \\ m_8 & m_9 & -m_8 & m_{10} \\ -m_7 & -m_8 & m_7 & -m_8 \\ m_8 & m_{10} & -m_8 & m_9 \end{bmatrix}, \tag{2}$$

where $k = L/2$, E is Young's modulus of elasticity and I_z is the section moment of inertia with respect to the z-axis,

$$\beta = \frac{EI}{\kappa G A k^2}. \tag{3}$$

κ is the shear correction factor, G is the shear modulus and A is the area of the cross-section of the element and

$$\begin{gathered} m_1 = 156 + 882\beta + 1260\beta^2, \qquad m_2 = (44 + 231\beta + 315\beta^2)k, \\ m_3 = 54 + 378\beta + 630\beta^2, \qquad m_4 = (-26 - 189\beta - 315\beta^2)k, \\ m_5 = (16 + 84\beta + 126\beta^2)k^2, \qquad m_6 = (-12 - 84\beta - 126\beta^2)k^2, \\ m_7 = 18, \qquad m_8 = (3 - 45\beta)k, \\ m_9 = (8 + 30\beta + 180\beta^2)k^2, \qquad m_{10} = (-2 - 30\beta + 90\beta^2)k^2. \end{gathered} \tag{4}$$

The stiffness and mass matrices for the 1 d.o.f. $\{u\}$ local axial displacement in the x direction are [21]

$$[K_2] = \frac{EA}{k}\begin{bmatrix} \frac{1}{2} & -\frac{1}{2} \\ -\frac{1}{2} & \frac{1}{2} \end{bmatrix}, \qquad [M_2] = \rho A k \begin{bmatrix} \frac{2}{3} & \frac{1}{3} \\ \frac{1}{3} & \frac{2}{3} \end{bmatrix}. \tag{5}$$

The resulting stiffness and mass matrices for all the 3 d.o.f.s. at each node incorporating the K_1, K_2, M_1 and M_2 matrices according to displacement vector δ are now

$$K_{el} = \begin{bmatrix} K_2 11 & & & K_2 12 & & \\ & K_1 11 & K_1 12 & & K_1 13 & K_1 14 \\ & K_1 21 & K_1 22 & & K_1 23 & K_1 24 \\ K_2 21 & & & K_2 22 & & \\ & K_1 31 & K_1 32 & & K_1 33 & K_1 34 \\ & K_1 41 & K_1 42 & & K_1 43 & K_1 44 \end{bmatrix}_{(6\times 6)} \tag{6}$$

and

$$M_{el} = \begin{bmatrix} M_2 11 & & & M_2 12 & & \\ & M_1 11 & M_1 12 & & M_1 13 & M_1 14 \\ & M_1 21 & M_1 22 & & M_1 23 & M_1 24 \\ M_2 21 & & & M_2 22 & & \\ & M_1 31 & M_1 32 & & M_1 33 & M_1 34 \\ & M_1 41 & M_1 42 & & M_1 43 & M_1 44 \end{bmatrix}_{(6\times 6)}. \tag{7}$$

2.2. THE STIFFNESS MATRIX FOR THE CRACK

According to St Venant's principle the stress field is influenced only in the region near to the crack. The additional strain energy due to the crack leads to flexibility coefficients expressed by stress intensity factors derived by means of Castigliano's theorem in the linear elastic range. The compliance coefficients are derived from the strain energy release rate, J, developed in Griffith–Irwin theory. For plane strain, J has the expression [22, 23]

$$J = \frac{(1-\nu^2)}{E} K_{\mathrm{I}}^2 + \frac{1-\nu^2}{E} K_{\mathrm{II}}^2 + \frac{(1+\nu)}{E} K_{\mathrm{III}}^2, \tag{8}$$

where E is the elastic modulus, ν the Poisson ratio and K_{I}, K_{II} and K_{III} are stress intensity factors for opening, sliding and tearing mode deformation respectively. When modes I and II are concerned, it is possible to give analytical expressions for the flexibility coefficients for a uniform beam with a rectangular cross-section. The superposition of the stress intensity factors, for the three types of loading shown in Figure 2, gives, for the strain energy release rate, the following expression:

$$J = \frac{1-\nu^2}{E^*} \{(K_{\mathrm{I}}(F) + K_{\mathrm{I}}(M))^2 + K_{\mathrm{II}}(Q)^2\} \tag{9}$$

with

$$\begin{aligned} K_{\mathrm{I}}(F) &= \frac{F}{bd}\sqrt{\pi a}\, F_1\left(\frac{a}{b}\right), \\ K_{\mathrm{I}}(M) &= \frac{6M}{b^2 d}\sqrt{\pi a}\, F_2\left(\frac{a}{b}\right), \\ K_{\mathrm{II}}(Q) &= \frac{\kappa Q}{bd}\sqrt{\pi a}\, F_3\left(\frac{a}{b}\right), \end{aligned} \tag{10}$$

and

$$F_1\left(\frac{a}{b}\right) = \sqrt{\frac{2b}{\pi a}\tan\left(\frac{\pi a}{2b}\right)}\,\frac{0{\cdot}752 + 2{\cdot}02(a/b) + 0{\cdot}37(1-\sin \pi a/2b)^3]}{\cos(\pi a/2b)},$$

$$F_2\left(\frac{a}{b}\right) = \sqrt{\frac{2b}{\pi a}\tan\left(\frac{\pi a}{2b}\right)}\frac{0.923 + 0.199(1 - \sin \pi a/2b)^4]}{\cos(\pi a/2b)}, \tag{11}$$

$$F_3\left(\frac{a}{b}\right) = \frac{[1{\cdot}122 - 0{\cdot}561(a/b) + 0{\cdot}085(a/b)^2 + 0{\cdot}180(a/b)^3]}{\sqrt{1 - a/b}},$$

where the coefficient κ is a numerical factor depending on the shape of the cross-section derived from Timoshenko beam theory, $E^* = E$ for plane strain and $E^* = E/(1 - \nu^2)$ for plane stress, and (a/b) is the relative depth of the crack. The contribution to the opening mode, mode I, is made by the bending moment M and the axial force F. The edge sliding mode, mode II, receives a contribution from the shear force Q. If U is the strain energy of a cracked structure with a crack area A under the load P_i, then

$$J = \frac{\partial U(P_i, A)}{\partial A}. \tag{12}$$

At the same time, Castigliano's theorem implies that the additional displacement due to crack, according to the direction of the P_i, is

$$u_i = \frac{\partial U(P_i, A)}{\partial P_i}. \tag{13}$$

Substituting the strain energy release rate J into equation (13) the relation between displacement and strain energy release rate J can be written as follows:

$$u_i = \frac{\partial}{\partial P_i}\int_A J(P_i, A)\,\mathrm{d}A. \tag{14}$$

The flexibility coefficients, which are functions of the crack shape and the stress intensity factors, can be introduced as follows [24, 25]:

$$c_{ij} = \frac{\partial u_i}{\partial P_j} = \frac{\partial^2}{\partial P_i \partial P_j}\int_A J(P_i, A)\,\mathrm{d}A, \quad i, j = 1, \ldots, 3, \quad P_1 = F, \quad P_2 = Q, \quad P_3 = M. \tag{15}$$

The compliance coefficients matrix, after being derived from the above equation, can be written according to the displacement vector $\delta = \{u, v, \theta\}$ as

$$C = \begin{bmatrix} c_{11} & 0 & c_{13} \\ 0 & c_{22} & 0 \\ c_{31} & 0 & c_{33} \end{bmatrix}_{(3x3)}. \tag{16}$$

The inverse of the compliance matrix C^{-1} is the stiffness matrix due to the crack. Finally, the resulting stiffness matrix for the crack can be given as

$$K_{cr} = \begin{bmatrix} [C]^{-1} & -[C]^{-1} \\ -[C]^{-1} & [C]^{-1} \end{bmatrix}_{(6x6)}. \tag{17}$$

2.3. CONTACT MODELLING

When two or more bodies come into contact, due to an externally applied loading, the contact region may increase or decrease, as with a closing crack, and these changing boundary conditions result in a non-linear contact problem which can be solved using the finite element method. In contact problems often no *a priori* information concerning the contact conditions is available, which presents considerable difficulties. In a contact analysis there are three possible states which are commonly assumed to occur: sticking, frictionless sliding and frictional sliding contact. It is also possible that a combination of these states could occur simultaneously in a single contact problem in different regions. The general objective, in a contact analysis, is to determine the contacting areas and contact pressures transmitted. In this study, contact analysis of the beam having an edge crack which is closing (seen in Figure 3) has been modelled using a proprietary finite element package.† The contact areas, pressures and overclosures provided by this package were used to synthesize the contact stiffnesses used in the coupling analysis of the component mode synthesis.

2.3.1. *Contact stiffness*

Consider a two-dimensional contact between two bodies as shown in Figure 4. Infinitesimal displacements in the normal and tangential directions (u_n, u_t) are independent. The contact itself can be idealized as two independent linear springs having stiffness k_n and k_t which are oriented in the normal and tangential directions.

When the normal force F_n is compressive the interface remains in contact and it is assumed that the normal displacements and forces respond as a linear spring. When the normal force F_n is tension the contact is broken and no force is transmitted. The change in normal displacement, assuming that there is no gap between bodies, can be given as

$$\Delta u_n = u_{n,B} - u_{n,A}, \tag{18}$$

where $u_{n,B}$ and $u_{n,A}$ are the displacements in the normal direction. The load–displacement curve can now be given as in Figure 5(a). Force in the tangent direction (F_t) is defined only when $F_n < 0$. When $|F_t| < \mu|F_n|$, where μ is the friction coefficient, there is no sliding at the interfaces and tangential displacements and forces respond as a linear spring. The relative displacement in the tangent direction, by assuming that there is no sliding, is

$$\Delta u_t = u_{t,B} - u_{t,A}, \tag{19}$$

where $u_{t,B}$ and $u_{t,A}$ are the displacements in the tangent direction. Figure 5(b) shows the load–displacement curve.

By using load–displacement relationships the contact stiffness for a nodal point, having 3 d.o.f.s, can be given as

$$K = [k_{ij}]_{(3\times 3)}, \tag{20}$$

where

$$k_{ij} = \frac{F_i}{\Delta u_j}, \quad i, j = 1, 2, 3, \tag{21}$$

†ABAQUS 5.5.

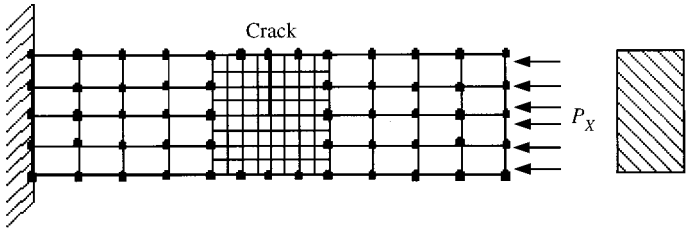

Figure 3. Finite element modelling of the cracked beam.

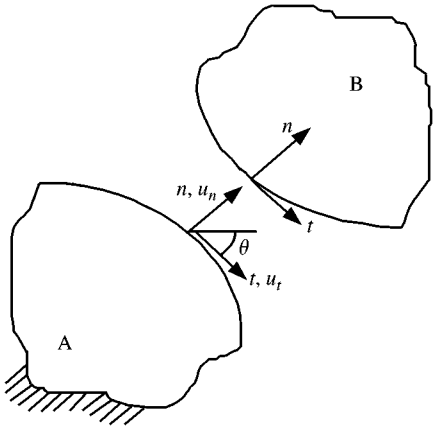

Figure 4. Contact between two bodies.

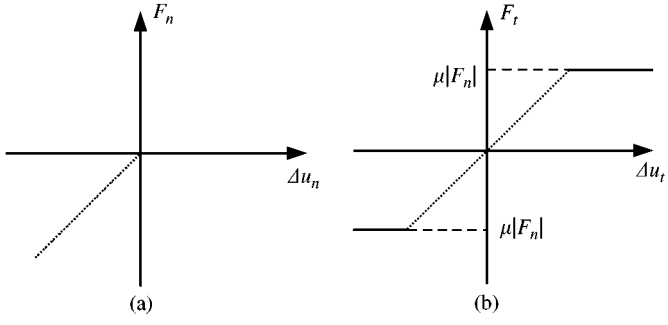

Figure 5. (a) Load–displacement curve for k_n; (b) load–displacement curve for k_t.

in which F_i and Δu_j are found, incrementally, by the proprietary finite element software. Finally, the additional contact stiffness due to the closing of the crack is given as

$$K_{con} = \begin{bmatrix} K & -K \\ -K & K \end{bmatrix}_{(6x6)}. \tag{22}$$

3. COMPONENT MODE ANALYSIS

Consider a component A. The equation of motion for this component is

$$M_A\ddot{q}_A + C_A\dot{q}_A + K_A q_A = f_A(t), \tag{23}$$

where M_A, C_A and K_A are mass, damping and stiffness matrices, respectively, for the component A, and q and $f_A(t)$ are the generalized displacement and external force vectors respectively. For undamped free vibration analysis, equation (23) becomes

$$M_A\ddot{q}_A + K_A q_A = f_A(t). \tag{24}$$

Assuming that

$$\{q\} = \{\phi\}\sin(\omega t + \beta), \quad \{\ddot{q}\} = -\omega^2\{\phi\}\sin(\omega t + \beta) \tag{25}$$

and substituting them into equation (24), results in the standard free vibration equation for the component A as

$$\omega_A^2 M_A \phi = K_A \phi, \tag{26}$$

which gives eigenvalues $\omega_{A1}^2, \ldots, \omega_{An}^2$ and modal matrix ϕ_A for the component A. Making the transformation, then

$$q_A = \phi_A p_A, \tag{27}$$

where p_A is the principal co-ordinate vector. By premultiplying ϕ_A^{T} and substituting equation (27), equation (24) becomes

$$(\phi_A^{\mathrm{T}} M_A \phi_A)\,\ddot{p}_A + (\phi_A^{\mathrm{T}} K_A \phi_A) p_A = \phi_A^{\mathrm{T}} f_A(t), \tag{28}$$

where

$$\phi_A^{\mathrm{T}} M_A \phi_A = [m_m], \qquad \phi_A^{\mathrm{T}} K_A \phi_A = [k_m], \tag{29}$$

with $[m_m]$ and $[k_m]$ being the modal mass and modal stiffness matrices respectively. Mass normalizing the modal matrix by

$$\psi_{ij} = \frac{\phi_{ij}}{\sqrt{m_{jj}}}, \tag{30}$$

where ψ_{ij} is mass normalized mode vector, and by using the following transformation:

$$q_A = \psi_A s_A \tag{31}$$

and by premultiplying ψ_A^{T} and substituting equation (31), equation (24) becomes

$$I\ddot{s}_A + \omega_A^2 s_A = \psi_A^{\mathrm{T}} f_A(t), \tag{32}$$

where ω_A^2 is a diagonal matrix comprising the eigenvalues of A.

3.1. COUPLING OF THE COMPONENTS

3.1.1. *Open crack*

Consider two components A and B connected together via springs, as illustrated in Figure 6. The kinetic and strain energy of the two components, in terms of principal modal co-ordinates, can be given as

$$T = \tfrac{1}{2}\dot{s}^{\mathrm{T}} M \dot{s}, \qquad U = \tfrac{1}{2} s^{\mathrm{T}} K s, \tag{33}$$

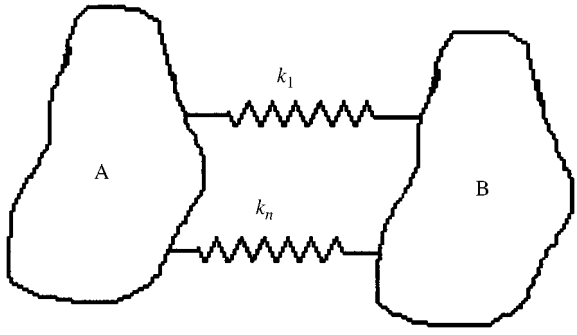

Figure 6. Two components connected by springs.

where T and U are kinetic and strain energy respectively. M and K in equation (33) are

$$M = \begin{bmatrix} I & 0 \\ 0 & I \end{bmatrix}, \qquad K = \begin{bmatrix} \omega_A^2 & 0 \\ 0 & \omega_B^2 \end{bmatrix}. \tag{34}$$

The strain energy of the connectors, in terms of principal modal co-ordinates, is

$$U_C = \tfrac{1}{2} s^{\mathrm{T}} \psi^{\mathrm{T}} K_C \psi s, \tag{35}$$

where K_C is the connector stiffness matrix comprising the stiffness matrix due to the crack. ψ in equation (35) can be written as

$$\psi = \begin{bmatrix} \psi_A & 0 \\ 0 & \psi_B \end{bmatrix}. \tag{36}$$

The total strain energy of the system is therefore,

$$U_T = \tfrac{1}{2} s^{\mathrm{T}} (K + \psi^{\mathrm{T}} K_{\mathrm{C}} \psi) s, \tag{37}$$

where K is the uncracked system stiffness which has been given by equation (34) and $(K + \psi^{\mathrm{T}} K_C \psi)$ is the system stiffness which includes stiffness due to the crack. By using Lagrange's equation, the equation of motion of the complete structure is

$$\ddot{s} + (K + \psi^{\mathrm{T}} K_C \psi) s = \psi^{\mathrm{T}} f(t), \tag{38}$$

where ψ has been given by equation (36), and $f(t)$ is the global force vector for the system.

3.1.2. *Closing crack*

When the crack closes, additional contact stiffness has to be taken into consideration. The strain energy of the connectors, in terms of principal modal co-ordinates, for a closing crack, can be given as

$$U_C = \tfrac{1}{2} s^{\mathrm{T}} \psi^{\mathrm{T}} [K_{C_i}] \psi s, \tag{39}$$

where K_{C_i} is the incremental connector stiffness matrix comprising the stiffness matrix due to crack K_{CR}, and the stiffness matrix due to contact K_{CON}, when the crack closes. K_{C_i} can be given as

$$[K_{C_i}] = \begin{bmatrix} \cdots & \cdots & \cdots \\ \cdots & [K_{CR}] + \lambda[K_{CON_i}] & \cdots \\ \cdots & \cdots & \cdots \end{bmatrix}_{(N \times N)} \tag{40}$$

where λ is a scalar factor depending on the state of the crack, open or closed and assumed to be as follows

$$\lambda = 0 \quad \text{for opening half-cycle,}$$

$$\lambda = 1 \quad \text{for closing half-cycle.} \tag{41}$$

The total strain energy of the system is given as,

$$U_T = \tfrac{1}{2} s^{\mathrm{T}}(K + {}^{\mathrm{T}}[K_{C_i}]\psi)s, \tag{42}$$

where $(K + \psi^{\mathrm{T}}[K_{C_i}]\psi)$ is the system stiffness which includes stiffness due to the crack and contact. Again, by using Lagrange's equation, the equation of motion of the complete structure can be given

$$\ddot{s} + (K + \psi^{\mathrm{T}}[K_{C_i}]\,\psi)s = \psi^{\mathrm{T}} f(t). \tag{43}$$

From equations (43) the eigenvalues and eigenvectors of the cracked system, for the case of a closing crack, can be determined. After solving these equations, the displacements for each component are calculated by using equation (31).

TABLE 1

Natural frequencies of the cracked beam for $\xi/L = 0{\cdot}20, 0{\cdot}40, 0{\cdot}60$ *and* $0{\cdot}80$ (*cack is open*)

Nat.freqs.	ξ/L ratio	a/b ratio 0·20	a/b ratio 0·40	a/b ratio 0·60	a/b ratio 0·80	Intact beam
1st mode	0·20	1020·137	966·9525	842·2205	551·0463	0037·0189
2nd mode	0·20	6457·396	6454·483	6448·175	6436·008	6458·3438
3rd mode	0·20	17872·91	17596·57	16944·56	15512·55	17960·564
4th mode	0·20	34553·13	33100·42	29796·26	25182·06	34995·429
1st mode	0·40	1030·095	1006·856	942·7322	724·2739	
2nd mode	0·40	6389·394	6174·539	5689·841	4728·978	
3rd mode	0·40	17844·86	17499·83	16792·25	15606·35	
4th mode	0·40	34866·97	34420·09	32971·51	29180·94	
1st mode	0·60	1035·284	1029·262	1010·864	920·7848	
2nd mode	0·60	6365·914	6071·655	5371·803	3798·216	
3rd mode	0·60	17807·94	17359·27	16478·82	15153·19	
4th mode	0·60	34895·50	34572·37	33710·43	31412·07	
1st mode	0·80	1036·884	1036·414	1034·943	1026·769	
2nd mode	0·80	6440·057	6375·921	6174·710	5169·264	
3rd mode	0·80	17758·61	17077·99	15286·83	11353·18	
4th mode	0·80	34393·87	32639·52	29529·79	26230·83	

4. RESULTS AND DISCUSSION

4.1. OPEN CRACK

The method described has been applied to a cracked Timoshenko beam as shown in Figure 1. The dimensions of the beam are $L = 0{\cdot}2$, $b = 0{\cdot}0078$ and $d = 0{\cdot}025$ *m*, chosen to enable comparison with the results in the literature. Calculations have been performed with the numerical values of $\rho = 7850\ \mathrm{kg/m^3}$, $E = 216 \times 10\ \mathrm{N/m^2}$, $G = 3E/8$ and $\nu = -0{\cdot}28$. In order to check the accuracy of the method, the four lowest natural frequencies for various crack positions and crack ratios are examined. In Table 1 the first four natural frequencies of the cracked Timoshenko beam and intact beam have been given for various crack positions and crack ratios. Figure 7 shows a plot of the ratio of the first natural frequency of the cracked beam to the first natural frequency of the corresponding intact Timoshenko beam as a function of the crack depth ratio a/b for several crack positions. The natural frequencies of the cracked beam are lower than the natural frequencies of the corresponding intact beam, as expected. These differences increase with the depth of the crack. Due to the

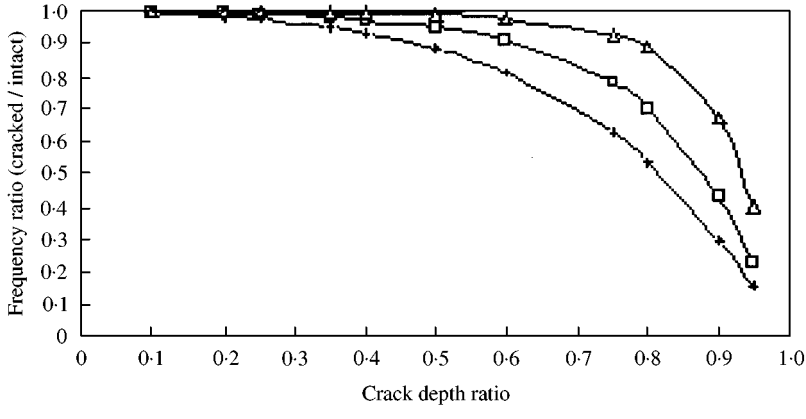

Figure 7. Frequency ratios for different crack positions (crack is open): —+—, $\xi = 0{\cdot}2$; —□—, $\xi = 0{\cdot}4$; —△—, $\xi = 0{\cdot}6$.

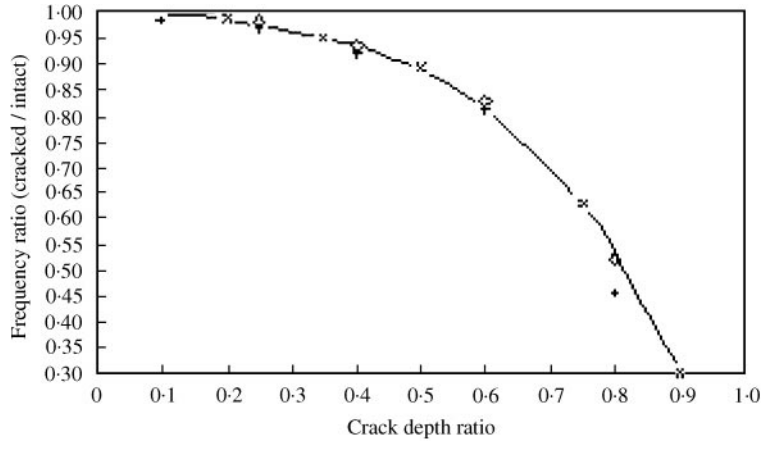

Figure 8. Change in the first natural frequency in terms of crack ratio (crack is open): ——, $\xi = 0{\cdot}2$; —×—, Abraham; —+—, Shen; —◇—, Wendtland.

bending moment along the beam, which is concentrated at the fixed end, a crack near the free end will have less effect on the fundamental frequency than a crack closer to the fixed end and it can be said that the frequencies are almost unchanged when the crack is located away from the fixed end.

In developing new methods of analysis it is important to benchmark against known experimental, theoretical and numerical cases. For this reason, the results are compared with the experimental data obtained by Wendtland [26] and theoretical data obtained by Abraham [27] and Shen and Pierre [28] as shown in Figures 8 and 9.

The first, second and third modes are shown in Figures 10, 11 and 12 for a crack respectively, at $\xi = 0{\cdot}2L$, $0{\cdot}4L$ and $0{\cdot}6L$ when the crack depth ratio takes the values $a/b = 0{\cdot}2$, $0{\cdot}4$ and $0{\cdot}6$.

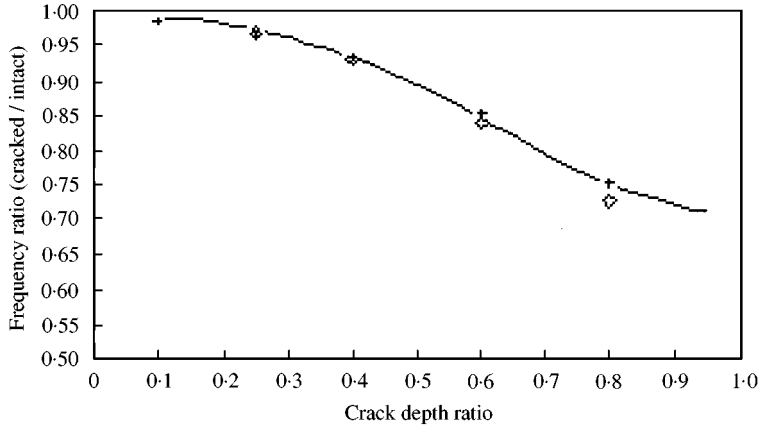

Figure 9. Change in the fourth natural frequency in terms of crack ratio (crack is open): ——, $\xi = 0{\cdot}8$; —+—, Shen; —◇—, Wendtland.

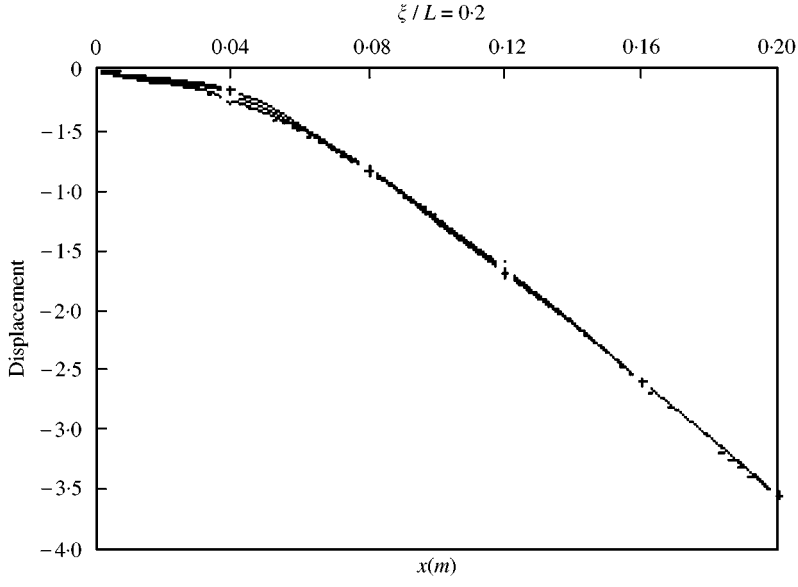

Figure 10. First-mode shapes of cracked beam for $\xi/L = 0{\cdot}2$ and $a/b = 0{\cdot}2$, $0{\cdot}4$, $0{\cdot}6$ (crack is open): ——, Intact; ---◇---, $a/b = 0{\cdot}2$; —□—, $a/b = 0{\cdot}4$; —+—, $a/b = 0{\cdot}6$.

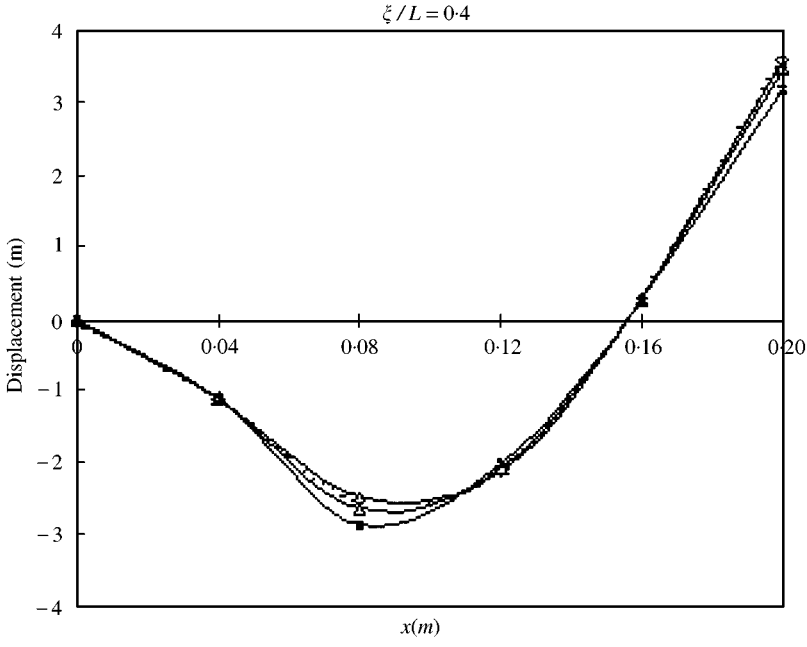

Figure 11. Second-mode shapes of cracked beam for $\xi/L = 0{\cdot}4$ and $a/b = 0{\cdot}2$, 0·4, 0·6 (crack is open): ——, Intact; ---◇---, $a/b = 0{\cdot}2$; —△—, $a/b = 0{\cdot}4$; —×—, $a/b = 0{\cdot}6$.

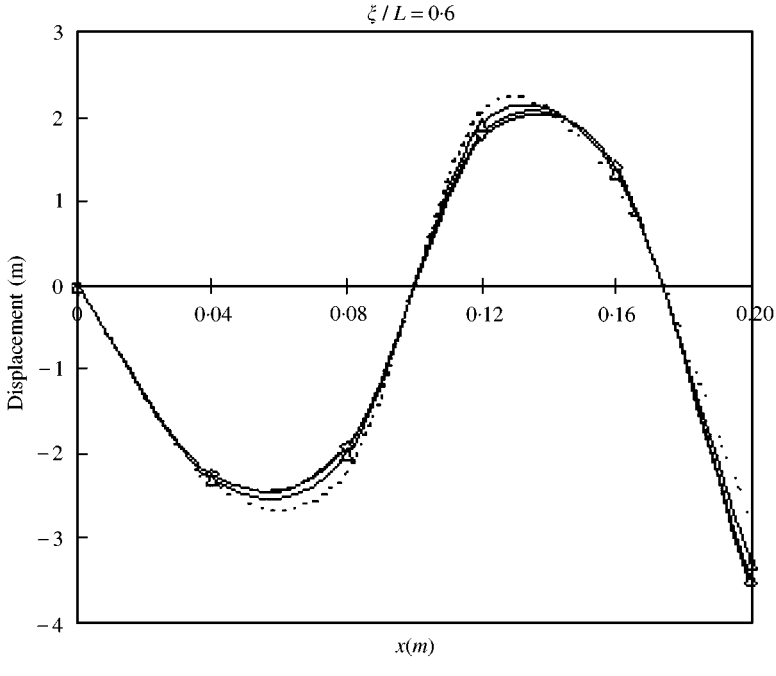

Figure 12. Third-mode shapes of cracked beam for $\xi/L = 0{\cdot}6$ and $a/b = 0{\cdot}2$, 0·4, 0·6 (crack is open): ——, Intact; ---◇---, $a/b = 0{\cdot}2$; —△—, $a/b = 0{\cdot}4$; $a/b = 0{\cdot}6$.

4.2. CLOSING CRACK

To facilitate comparison, the properties of the Timoshenko beam are the same as those used by Abraham [27] ($L = 3$, $b = 0{\cdot}2$ and $d = 0{\cdot}2$ m). The crack parameters are $\xi = 0{\cdot}5/L$ and $a/b = 0{\cdot}5$. As analysis has been done incrementally the crack face will come into contact progressively. The contact stiffness, for each increment, calculated and corresponding eigenvalues and mode shapes obtained. Tables 2–5 give the natural frequencies for the closing crack and for the corresponding open crack and intact beam. As expected the natural frequencies lie between the natural frequencies of the intact beam and those obtained by the model of the open crack. This is due to the fact that the global stiffness of the system is between the stiffnesses for the open crack and intact beam cases, whilst the inertia distribution is unchanged.

As can be seen from Figures 13 and 14, there is a good agreement between results obtained by current method and by the method given by reference [27], in which the analysis has been done by a simplified analytical solution [20]. When the crack closes there is an increase in the natural frequencies since the system stiffness increases due to contact effects.

TABLE 2

Natural frequencies of the first increment when 10% *of the crack surfaces are closed*

Natural frequencies for $a/b = 0{\cdot}5$ *and* $\xi = 0{\cdot}5/L$		
Intact beam	Open crack	First increment
117·913749217	112·205673906	115·553127158
724·825104081	610·542787398	669·823316719
1976·19407474	1972·90087756	1974·00435129

TABLE 3

Natural frequencies of the third increment when 30% *of the crack surfaces are closed*

Natural frequencies for $a/b = 0{\cdot}5$ and $\xi = 0{\cdot}5/L$		
Intact beam	Open crack	Third increment
117·913749217	112·205673906	115·598945934
724·825104081	610·542787398	670·770766303
1976·19407474	1972·90087756	1974·02048400

TABLE 4

Natural frequencies of the fifth increment when 80% *of the crack surfaces are closed*

Natural frequencies for $a/b = 0{\cdot}5$ and $\xi = 0{\cdot}5/L$		
Intact beam	Open crack	Fifth increment
117·913749217	112·205673906	115·871022308
724·825104081	610·542787398	676·486346856
1976·19407474	1972·90087756	1974·11689350

TABLE 5

Natural frequencies of the sixth increment when 80% of the crack surfaces are closed

Natural frequencies for $a/b = 0{\cdot}5$ and $\xi = 0{\cdot}5/L$		
Intact beam	Open crack	Sixth increment
117·913749217	112·205673906	115·894440482
724·825104081	610·542787398	676·985583037
1976·19407474	1972·90087756	1974·12524094

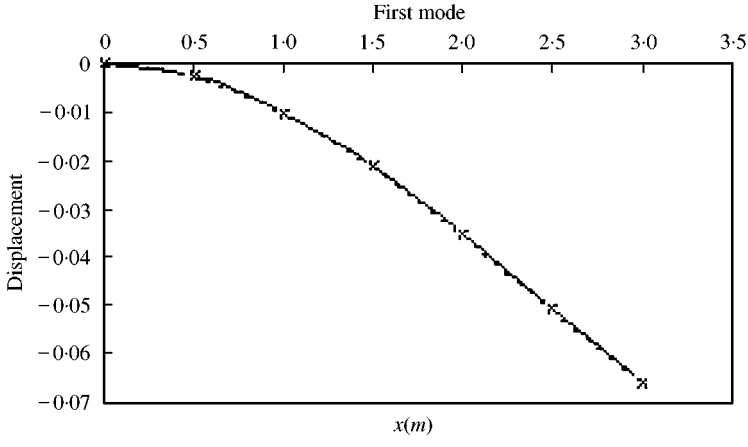

Figure 13. First-mode shapes when crack is fully closed, $\xi/L = 0{\cdot}5$ and $a/b = 0{\cdot}5$: - - - - -, present method; —×—, Abraham.

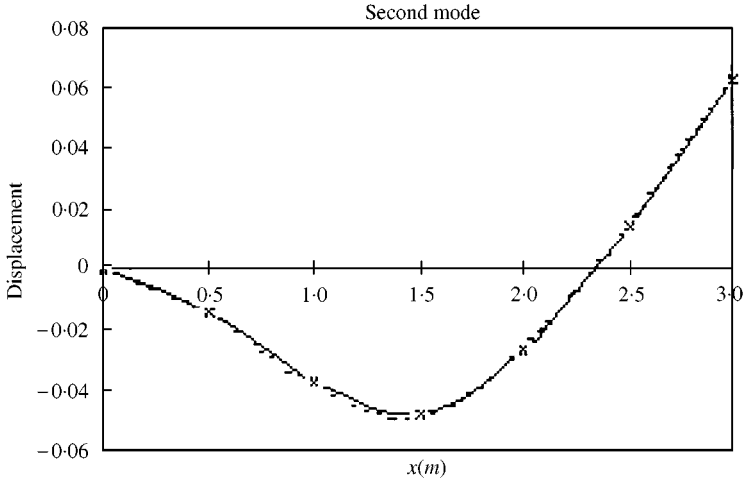

Figure 14. Second-mode shapes when crack is fully closed, $\xi/L = 0{\cdot}5$ and $a/b = 0{\cdot}5$: - - - - -, present method; —×—, Abraham.

5. CONCLUDING REMARKS

Previous work by Abraham and Brandon [19, 20] was based on a hybrid approach using mode superposition when a cracked structure was in either the open-crack or closed-crack

condition but adopting a time-domain approach during the brief intervals of transition. Experience of these methods suggested that a more sophisticated modelling approach during the transition intervals would enable the simulation to be achieved using an evolving modal model without the necessity to transform to the time domain and give significant insights into the evolution of the non-linear behaviour of the system.

The availability of a library of eigensystems corresponding to different degrees of closure potentially enables the mode superposition scheme to be extended into the transition interval.

REFERENCES

1. R. D. ADAMS and P. CAWLEY 1985 *The Shock and Vibration Bulletin*, Part 3. Naval Research Laboratory, Washington, DC. Vibration techniques in nondestructive testing.
2. N. STUBBS 1985 *2nd International Symposium on Structural Control, University of Waterloo, Waterloo, Ontario, Canada*, 15–17 *July* 1985, Vol. 2, 694–713. A general theory of non-destuctive damage detection in structures.
3. F. D. JU and M. E. MIMOVICH 1988 *ASME Journal of Vibration, Acoustics, Stress and Reliability in Design* **110**, 456–463. Experimental diagnosis of fracture damage in structures by the modal frequency method.
4. A. K. PANDEY, M. BISWAS and M. M. SAMMAN 1991 *Journal of Sound and Vibration* **145**, 321–332. Damage detection from changes in curvature mode shapes.
5. M. A. AKGUN and F. D. JU 1990 *Journal of Mechanical Structures and Machinery* **18**, 175–196. Damage diagnosis in frame structures with a dynamic response method.
6. R. L. CARLSON 1974 *Experimental Mechanics* **14**, 452–458. An experimental study of the parametric excitation of a tensioned sheet with a cracklike opening.
7. P. GUDMUNDSON 1983 *Journal of Mechanics Physics Solids* **31**, 329–345. The dynamic behaviour of slender structures with cross-sectional cracks.
8. A. IBRAHIM, F. ISMAIL and H. R. MARTIN 1987 *Journal of Analytical, Experimental Modal Analysis* **2**, 76–82. Modelling of the dynamics of continuous beam including nonlinear fatigue crack.
9. L. W. CHEN and C. L. CHEN 1988 *Computers and Structures* **28**, 67–74. Vibration and stability of cracked thick rotating blades.
10. R. ACTIS and A. D. DIMAROGONAS 1989 *12th ASME Conference on Mechanical Engineering, Vibration and Noise, Montreal, Canada, September* 1989, Vol. 18, 99–104. Non-linear effects due to closing cracks in vibrating beams.
11. K. R. COLLINS, P. H. PLAUT and P. H. WAUER 1992 *ASME Journal of Vibration and Acoustics* **114**, 171–177. Free and forced longitudinal vibrations of a cantilevered bar with a crack.
12. M. I. FRISWELL and J. E. T. PENNY 1992 *10th International Modal Analysis Conference, San Diego, CA*, 516–521. A simple nonlinear model of a cracked beam.
13. R. GASH, M. PERSOM and B. WEITZ 1988 *Proceedings of the Conference Vibrations in Rotating Machinery, Edingburgh, England, C*314/88. Dynamic behaviour of the Laval rotor with a cracked hollow shaft.
14. C. A. PAPADOPOULOS and A. D. DIMAROGONAS 1988 *ASME Journal of Vibration, Acoustics, Stress, and Reliability in Design* **110**, 356–359. Stability of cracked rotors in the coupled vibration mode.
15. B. ZASTRAU 1985 *Archiv of Mechanics* **37**, 731–743. Vibrations of cracked structures.
16. G. L. QIAN and J. S. JIANG 1990 *Journal of Sound and Vibration* **138**, 233–243. The dynamic behaviour and crack detection of a beam with a crack.
17. W. OSTACHOWICZ and M. KRAWCZUK 1990 *Computers and Structures* **36**, 245–250. Vibration analysis of a cracked beam.
18. M. KRAWCZUK and W. OSTACHOWICZ 1994 *Proceedings of the 19th International Seminar on Modal Analysis, K.U. Leuven, Belgium*, Vol. 3, 1067–1078. Forced vibrations of a cantilever Timoshenko beam with a closing crack.
19. O. N. L. ABRAHAM and J. A. BRANDON 1995 *Transactions of the American Society of Mechanical Engineers: Journal of Vibration and Acoustics* **117**, 370–377. The modelling of the opening and closing of a crack.

20. J. A. BRANDON and O. N. L. ABRAHAM 1995 *Journal of Sound and Vibration*, **185**, 415–430. Counter-intuitive quasi-periodic motion in the autonomous vibration of cracked Timoshenko beams.
21. M. PETYT 1990 *Introduction to Finite Element Vibration Analysis*. Great Britain: Cambridge University Press.
22. G. IRWIN 1960 *Fracture Mechanics*, *Structural Mechanics* (J. N. Goodier and N. J. Hoff) editors New York: Pergamon Press.
23. H. TADA, P. C. PARIS and G. R. IRWIN 1985 *The Stress Analysis of Cracks Handbook*. St. Louis, MI: Paris production incorporated and Del Research Corporation, second edition.
24. DIMAROGONAS and S. A. PAIPETIS 1983 *Analytical Methods in Rotor Dynamics*. Barking, England: Applied Science Publishers.
25. C. A. PAPADOPOULOS and A. D. DIMAROGONAS 1988 *ASME Journal of Vibration, Acoustics, Stress, and Reliability in Design* **110**, 1–8. Coupled longitudinal and bending vibrations of a cracked shaft.
26. D. WENDTLAND 1972 *Ph.D. thesis*, *Universitat Karlsruhe*. Anderungen der Biegeeigenfrequenzen einer idealisierten schaufel durc risse.
27. O. N. L. ABRAHAM 1993 *Ph.D. thesis*, *University of Wales College of Cardiff*. Dynamic modelling of cracked Timoshenko beams.
28. M. H. H. SHEN and C. PIERRE 1990 *Journal of Sound and Vibration* **138**, 115–134. Natural modes of Bernoulli–Euler beams with symmetric cracks.